Heliyon 9 (2023) e21069

Contents lists available at ScienceDirect

Heliyon

journal homepage: www.cell.com/heliyon

Differential effects of climatic and non-climatic factors on the distribution of vegetation phenology trends on the Tibetan plateau

Xianglin Huang [a,b,e], Ru An [a,*], Huilin Wang [c,**], Fei Xing [b], Benlin Wang [d], Mengyao Fan [b], Yunying Fang [e], Hongliang Lu [b]

[a] College of Hydrology and Water Resources, Hohai University, Nanjing, 210024, China
[b] School of Earth Science and Engineering, Hohai University, Nanjing, 211100, China
[c] Department of Geography Information Science, Nanjing University, Nanjing, 210023, China
[d] School of Geographic Information and Tourism, Chuzhou University, Chuzhou, 239000, China
[e] Australian Rivers Institute, Griffith University, Queensland, 4111, Australia

ARTICLE INFO

Keywords:
Phenology
Tibetan plateau
Geographical detector
Climatic factors
Non climatic factors

ABSTRACT

The study of vegetation phenology changes is important because it is a sensitive indicator of climate change, affecting the exchange of carbon, energy and water fluxes between the land and the atmosphere. Previous studies have focused on the effects of climatic factors among environmental factors on vegetation phenology, thus the effects of non-climatic factors among environmental factors have not been well quantified. This study endeavors to scrutinize the spatiotemporal inconsistency in the start-of-season (SOS) and the end-of-season (EOS) on the Tibetan Plateau (TP) and to quantify the effects of environmental factors on phenology. To this end, the Moderate-resolution Imaging Spectroradiomater (MODIS) Normalized Difference Vegetation Index (NDVI) data from 2001 to 2018 and four common used methods were employed to extract SOS and EOS, and the site data was used to select the most appropriate phenology results. The Geodetector model was used to assess and measure the explanatory power of different environmental factors. The research results indicate that temperature exerts a more substantial impact on phenology than precipitation on TP. non-climatic factors such as longitude, latitude, and elevation are more influential in determining the distribution of phenological trends than climatic factors. Among these non-climatic factors, latitude has the most prominent effect on the trends of SOS. Furthermore, non-climatic factors exhibit a stronger effect on SOS, whereas EOS is more susceptible to climatic factors and less influenced by non-climatic factors. These discoveries bear great significance in comprehending the intricate outcomes of regional changes on vegetation phenology and enhancing phenology models.

1. Introduction

Vegetation phenology is essentially a study of the relationship between plant growth and development and environmental factors, which can visually reflect changes in the natural environment and indicate the adaptation of plants to environmental changes [1–3]. Since the 20th century, global warming has had a profound impact on vegetation phenology in various regions [3,4], and the

* Corresponding author.
** Corresponding author.
E-mail addresses: anrunj@hhu.edu.cn (R. An), huilin_wang@163.com (H. Wang).

https://doi.org/10.1016/j.heliyon.2023.e21069
Received 19 April 2023; Received in revised form 13 October 2023; Accepted 13 October 2023
Available online 14 October 2023

advantage of being easily observable has made phenology a sensitive indicator of climate change [5,6]. Therefore, a comprehensive and accurate conception of the influence of climatic and non-climatic factors on phenological change trends is essential to deepen the understanding of the feedback mechanisms of vegetation to climate and future ecosystem dynamics.

The overall process of a growing season from sowing, germination, maturation, and defoliation of plants is described by phenology [7]. The accuracy of remote sensing methods for extracting phenological parameters is influenced by two key points, one for smoothing of time series data and the other for the determination of phenological indicators [8]. Numerous methods have been applied to extract phenological indicators from remote sensing products, mainly including the threshold method [9,10], delayed moving average method [11], the maximum slope of change method [12], logistic curve fitting method [13], dynamic threshold method [14–16], and the seasonal trend decomposition by LOESS (STL) [17], etc. To make the phenology results more reasonable, this paper adopts the tempo-differentially selected growth rate model (TDSGM) for the extraction of phenology indicators [18].

The climate impacts on vegetation phenology have received increasing attention as global warming has intensified. In extreme drought years, the start-of-season (SOS) was advanced and the end-of-season (EOS) was delayed in most regions compared to normal years [19]. Researchers found that SOS in the northern hemisphere was earlier and EOS was later, while temperature was thought to be the main cause of vegetation phenology changes [1,20]. According to previous studies, higher spring temperatures could lead to an earlier onset of phenological events [21], and global warming had a significant impact on spring phenology [22]. It was also shown that in temperate or cold regions, especially in areas with less precipitation in winter, cumulative precipitation in late winter and early spring had a higher effect on SOS than temperature [23]. In particular, the effect of precipitation on vegetation phenology was more significant in arid or semi-arid regions [24]. However, non-climatic factors might also have influenced vegetation phenology. Spring phenology always showed a clear latitudinal pattern due to the variation of temperature with latitude [25]. And studies on vegetation phenology in the Source Region of the Yellow River found that EOS was closely related to elevation [26].

In addition, most of the recent investigations on the relationship between phenology and influence factors used partial correlation analysis [27,28], least squares regression [29,30] and multiple regression analysis [22,31]. However, these methods have limitations in studying the effects of non-climatic and climatic factors on phenology at the same research scale. In this study, we examined the effects of climatic and non-climatic factors on vegetation phenology changes. For climatic factors, we selected temperature and precipitation data from all four seasons. For non-climatic factors, we considered elevation, longitude, latitude, soil type, slope, and aspect. We employed the geographical detector model for our analysis. Geodetector is a statistical method to detect spatial differentiation, as well as to reveal the driving forces behind it. The advantage is that the relative importance between the drivers of phenological variability can be quantified, while eliminating the need to follow the assumption of linearity and multiple covariances between drivers of traditional methods [32,33]. The model has been successfully applied to determine the influence of climatic factors and anthropogenic factors on vegetation change [32–36]. In this study, the contributions of both climatic and non-climatic factors to vegetation phenology were analyzed. The spatial variability of the primary factors influencing phenological changes was explored. Additionally, a detailed analysis was conducted on phenological change trends across different spatial zones defined by these influencing factors.

As the "Third Pole of the Earth" and "Water Tower of Asia", the TP is the origin of major rivers in China [37]. In recent times, it has undergone drastic climate change that is markedly higher than the global average during the same period, leading to a significant escalation of ecological risks confronting the plateau [25]. The phenological variations in the vegetation of the plateau have piqued the interest of numerous scholars. Nevertheless, current research on vegetation phenology has predominantly focused on the direct impact of climatic factors such as temperature and precipitation on vegetation phenology [1,20]. Differences in the spatial position of vegetation engender discrepancies in the surrounding environmental conditions, which indirectly influence vegetation phenology.

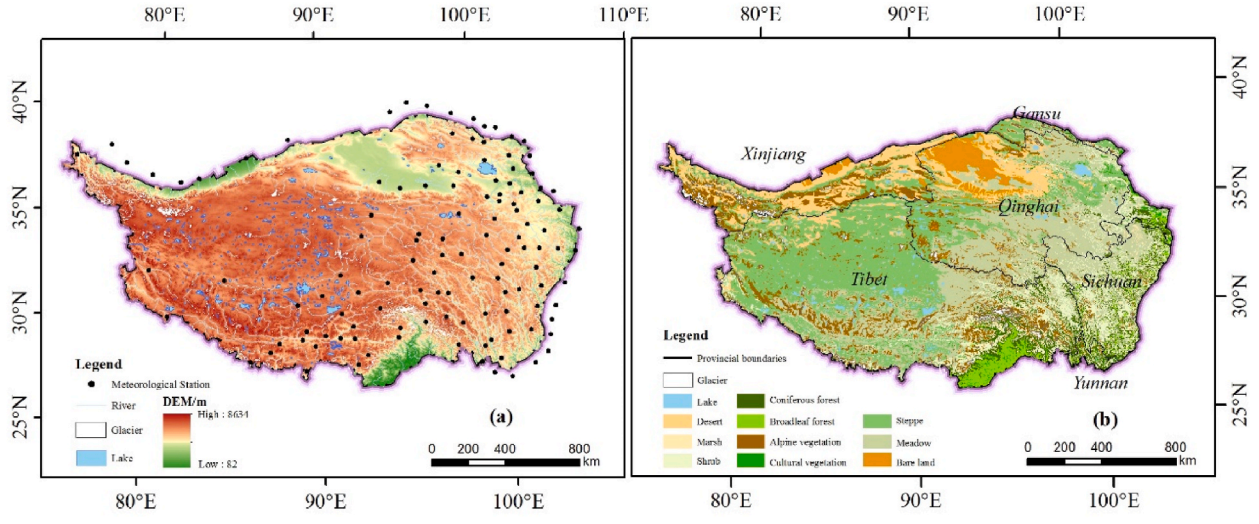

Fig. 1. Elevation and vegetation types of the TP.

However, the effect of these non-climatic factors on vegetation phenology trends remains ambiguous in prior research, and few have compared the direct and indirect impact of climatic and non-climatic factors on vegetation phenology trends. Our objectives encompass three aspects: (1) to scrutinize the temporal and spatial designs of vegetation phenology indicators on the Tibetan Plateau (TP), (2) to quantitatively analyze the influence of climatic and non-climatic factors on the distribution of vegetation phenology trends and investigate the sensitivity of various phenology indicators to climatic and non-climatic factors, and (3) to explore the impact of climate factors on different vegetation phenology during different seasons, and determine the range of mean values of multi-year climate factors that promote vegetation SOS advancement and EOS delay, as well as the range and type of non-climate factors.

2. Materials and methods

2.1. Study area

The TP (80–105° E, 27–37° N) is located in southwest China. The region has an average elevation exceeding 4000 m above sea level. Stretching approximately 2800 km from east to west, it varies in width from 300 to 1500 km from north to south (Fig. 1a). Moreover, the TP, as the third pole of the Earth, is at the biological limit of hydrothermal conditions, and the plateau ecosystem is extremely fragile [38], which is extremely sensitive to the perturbation of climate change [39,40]. The hydrothermal environment of the TP exhibits the characteristics of cold and arid in the northwest, warm and humid in the southeast, cold at high altitudes and hot and humid at low altitudes. It makes the vegetation type of the TP show a horizontal-vertical geographical differentiation pattern (Fig. 1b). Cultivated plants whose phenological characteristics are easily disturbed by the human intervention were not considered in this study. Pixels with annual mean NDVI values (2001–2018) < 0.1 were also removed to prevent interference from non-vegetation signals [41].

2.2. Data source and preprocessing

2.2.1. NDVI data

The annual vegetation phenology data on the TP was determined from the Moderate-resolution Imaging Spectroradiometer (MODIS) normalized difference vegetation index (NDVI) dataset. In the study of vegetation phenology on the TP. MOD09A1 dataset product was obtained through the NASA Land Processes Distributed Active Archive Center (NLPDAAC, http://LPDAAC.usgs.gov). MOD09A1 NDVI data were used for this study [42]. The MODIS Reprojection Tool (MRT) was used for mosaic and reprojection analysis to generate 1 km spatial resolution data. Finally, the data were extracted using the boundary of the study area.

2.2.2. Climate data

The climate dataset for this study was derived from the spatially interpolated dataset of 1 km per 8 days fine gridded meteorological data nationwide from 2000 to 2018 published by National Ecosystem Science Data Center, National Science & Technology Infrastructure of China (http://www.nesdc.org.cn).

2.2.3. Ground-based phenological observations

Ground-based observations were obtained from 16 phenological stations of the Qinghai Meteorological Information Center (Table 1). The phenology data were recorded by manual observation, including station name, identification number, longitude, latitude, elevation, SOS and EOS. Strict protocols for phenological observations were established during the observation process [18].

Table 1
Phenological sites.

Station	Identification number	Latitude (N)	Longitude (E)	Elevation (m)
Xinghai	52943	35°35′	99°59′	3324
Tongde	52957	35°16′	100°39′	3290
Zeku	52968	35°02′	101°28′	3663
Tuotuohe	56004	34°13′	92°26′	4534
Zhiduo	56016	33°51′	95°36′	4184
Zaduo	56018	32°54′	95°18′	4068
Qumalai	56021	34°08′	95°47′	4176
Maduo	56033	34°55′	98°13′	4273
Qingshuihe	56034	33°48′	97°08′	4417
Maqin	56043	34°28′	100°15′	3720
Gande	56045	33°58′	99°54′	4051
Dari	56046	33°45′	99°39′	3968
Henan	56065	34°44′	101°36′	3501
Jiuzhi	56067	33°26′	101°29′	3630
Nangqian	56125	32°12′	96°29′	3645
Banma	56151	32°56′	100°45′	3530

2.2.4. Soil type and vegetation type

The soil texture dataset for the Qinghai-Tibet Plateau (2010) was extracted from the World Soil Database. This dataset was in a grid format and used the WGS84 projection. The primary soil classification system adopted was FAO-90, with the main soil types in this study being CMi, LPe, LPm, LPi, and LVh. Meanwhile, the vegetation type dataset was sourced from the 1:1 million China vegetation map. The primary vegetation types under study were meadow, steppe, shrubland, alpine vegetation, broadleaf forest, and coniferous forest. Both datasets were obtained from the National Tibetan Plateau Data Center (http://data.tpdc.ac.cn). Lastly, data corresponding to the study area was extracted using its boundaries.

2.3. Tempo-differentially selected growth rate model (TDSGM) and accuracy verification

2.3.1. The principle of TDSGM

The plant growth rate includes absolute growth rate (AGR) and relative growth rate (RGR) [43]. AGR refers to the absolute increase in plant weight, volume and height per unit of time. RGR is the percentage of increment per unit of time compared to the original amount [44]. According to the vegetation growth principle, the relative growth rate (RGR) of vegetation, was described as

$$q_2 = q_1 * e^{RGR*(t_2-t_1)} \tag{1}$$

where q_1 represents the dry mass of vegetation at time t_1, q_2 represents the dry mass of vegetation at time t_2, and e is the base of the natural logarithm (2.718).

The RGR is the relative growth rate of vegetation dry weight growth from time t_1 to time t_2. The NDVI can be used to represent the vegetation growth state [18]. Applying Eq. (1) to NDVI, we get

$$RGR = \frac{\ln q_2 - \ln q_1}{t_2 - t_1} = \ln NDVI_{t+1} - \ln NDVI_t \quad (t = 1, 2, 3, \ldots, 364) \tag{2}$$

where $NDVI_t$ and $NDVI_{t+1}$ denote the NDVI values on day t and day t+1, respectively, and t represents the specific number of days. The time corresponding to the maximum value of RGR represents the SOS.

By extending the original model [45], the relationship between RGR and AGR was found, and the absolute vegetation growth rate was

$$AGR = NDVI * \ln \frac{NDVI_t}{NDVI_{t-1}} \quad (t = 1, 2, 3, \ldots, 364) \tag{3}$$

where $NDVI_{t-1}$ and $NDVI_t$ are the NDVI values at day t-1 and day t, respectively. The time corresponding to the AGR maximum represents the EOS.

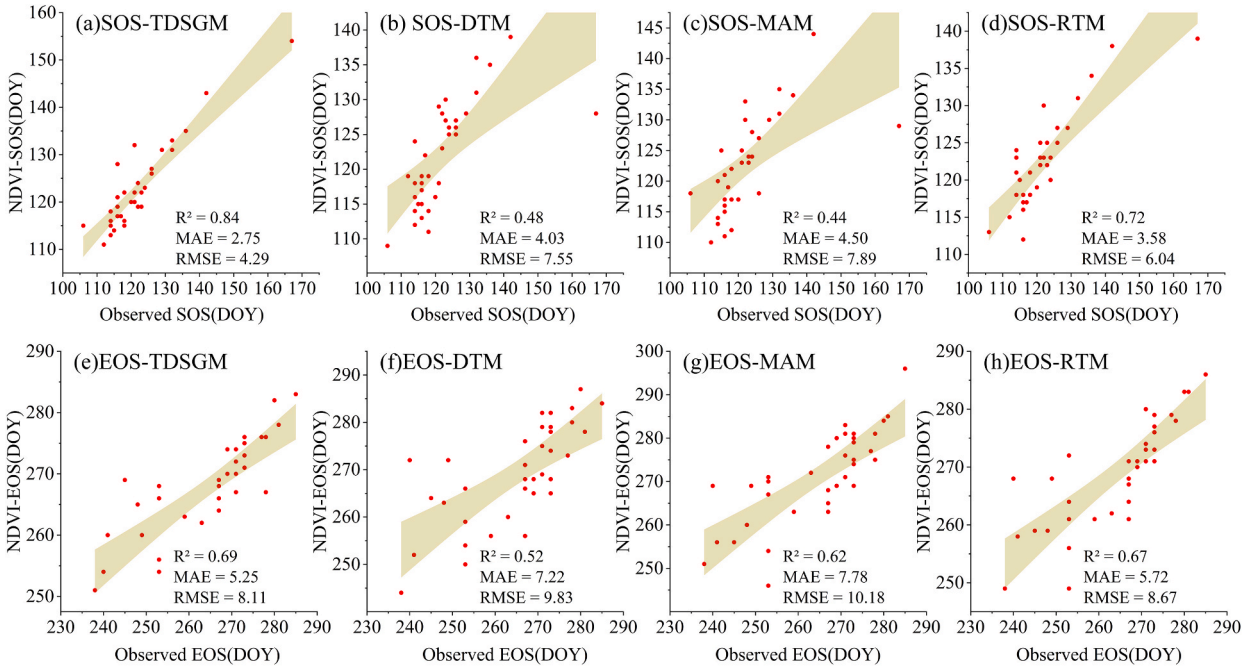

Fig. 2. Comparison of satellite-derived phenology data with ground-based phenology data: (a–d) SOS; (e–h) EOS.

2.3.2. Phenology metrics extraction and accuracy verification

Compared with three mainstream algorithms, namely the dynamic threshold method (DTM), ratio threshold method (RTM) and moving average method (MAM), this study adopted the TDSGM that extracts the vegetation phenology on the TP [18]. (1) The dynamic threshold method is an obvious improvement on the threshold method. It replaces the fixed threshold with a dynamic one, thus eliminating the influence of different soil background values and vegetation types. Although the dynamic threshold method fully takes into account the characteristics of vegetation index curves, its threshold selection varies depending on vegetation type and regional extent, and the dynamic threshold setting still needs to be set manually based on experience, which is easily influenced by subjective factors [9,14]. (2) The method of maximum slope of change determines the time of SOS and EOS in the vegetation growth process based on the first-order inverse of the vegetation index time series curve (slope of the curve). When the slope reaches its maximum in a year, it is defined as the SOS, and when the slope decreases to its minimum, it is defined as the EOS. This method is suitable for the extraction of vegetation phenology which is stable and less influenced by external conditions, but the accuracy of the inversion decreases when external conditions influence the vegetation phenology [12]. (3) The moving average method uses the intersection of the original NDVI curve and its moving average curve to determine the vegetation phenological period. The moving average method is more stable and reliable for the calculation of NDVI time series data with only one growing season in a year, but it is less effective for the identification of areas with multiple growing seasons or obvious response to rainfall in a year, because the selection of time interval may prevent the monitoring of the first greening period, and the moving average method is more sensitive to the setting of moving window [11]. The phenological dates were converted into Julian days, the cumulative number of days of the year (DOY).

The SOS and EOS extracted by the four methods were validated with observations from the geopotential stations, and the results showed that the accuracy of SOS and EOS extracted by the TDSGM on the TP was better than that of the dynamic threshold method, the ratio threshold method, and the moving average method (Fig. 2a–h). Moreover, the mean values of SOS and EOS obtained using remotely sensed data are higher than those from the site.

2.4. Trend analysis

We analyzed the spatial and temporal variation trends of phenological metrics at each pixel from 2000 to 2018 by unary linear regression. The rates of change of the time series are as follows

$$slope = \frac{n * \sum_{i=1}^{n} (i * T_i) - \sum_{i=1}^{n} i \sum_{i=1}^{n} T_i}{n * \sum_{i=1}^{n} i^2 - \left(\sum_{i=1}^{n} i\right)^2} \tag{4}$$

where the *slope* is the rate of change of SOS and EOS, T_i is the SOS or EOS of the *i*–th year, *i* is the sequence number, and *n* is the total number of years studied.

2.5. GeoDetector model

We obtained the explanatory power of climatic and non-climatic factors on the variation of phenology by the GeoDetector model, where climatic and non-climatic factors are independent variables, and the rate of change of the phenology is the dependent variable. Temperature and precipitation in four seasons were selected as climatic factors, and longitude, latitude, elevation, slope, aspect and soil type were selected as non-climatic factors (Table 2). Numerous studies found that climatic factors such as temperature and precipitation have a lagging and cumulative effect on vegetation growth [46]. Therefore, in this study, the main seasons considered when studying SOS and climate factors were the previous year's summer, the previous year's autumn, the previous year's winter, and the current year's spring. The main seasons considered when studying EOS and climate factors were the current year's spring, the current

Table 2
The environmental factors applied in this study, including climatic and non-climatic factors.

Classification	Name	ID	Unit
Climatic factors	Average spring temperature	Tem_Spring	°C
	Average summer temperature	Tem_Summer	°C
	Average autumn temperature	Tem_Autumn	°C
	Average winter temperature	Tem_Winter	°C
	Accumulated spring precipitation	Pre_Spring	mm
	Accumulated summer precipitation	Pre_Summer	mm
	Accumulated autumn precipitation	Pre_Autumn	mm
	Accumulated winter precipitation	Pre_Winter	mm
Non-climatic factors	Longitude	Longitude	°
	Latitude	Latitude	°
	Elevation	Elevation	m
	Slope	Slope	°
	Aspect	Aspect	–
	Soil type	Soil	–

year's summer, the current year's autumn, and the previous year's winter. The four seasons of the Qinghai Tibet Plateau are divided into spring (March–May), summer (June–August), autumn (September–November) and winter (December–February of the next year) [47].

The higher Q values of explanatory variables (independent variables) in GeoDetector model indicate that the spatial distribution pattern of the variable tends to be more similar to the spatial pattern of the response variable (dependent variable) [34–36]. The independent variables in this study include climatic and non-climatic factors, and the dependent variables include the trends of SOS and EOS. The Q values of the explanatory variables are calculated as follows

$$Q = 1 - \frac{\sum_{h=1}^{L} N_h \sigma_h^2}{N\sigma} = 1 - \frac{SSW}{SST} \quad (h = 1, 2, 3, \ldots, L)$$
$$SSW = \sum_{h=1}^{L} N_h \sigma_h^2, SST = N\sigma^2 \tag{5}$$

where h is the classification of the independent variable; L is the maximum number of classifications; N_h and N are the number of units within h and the whole region, respectively, and σ_h^2 and σ^2 are the variance of h and the whole region, respectively. SSW and SST are within the sum of squares and the total sum of squares for the whole region, separately.

As shown in Fig. 3, the original data of the independent and dependent variables are raster data, while the data types of the independent variables are categorized into categorical and continuous variables. The optimal discretization framework is used to select the optimal discretization solution, which discretizes the continuous variables and converts them into the corresponding categorical

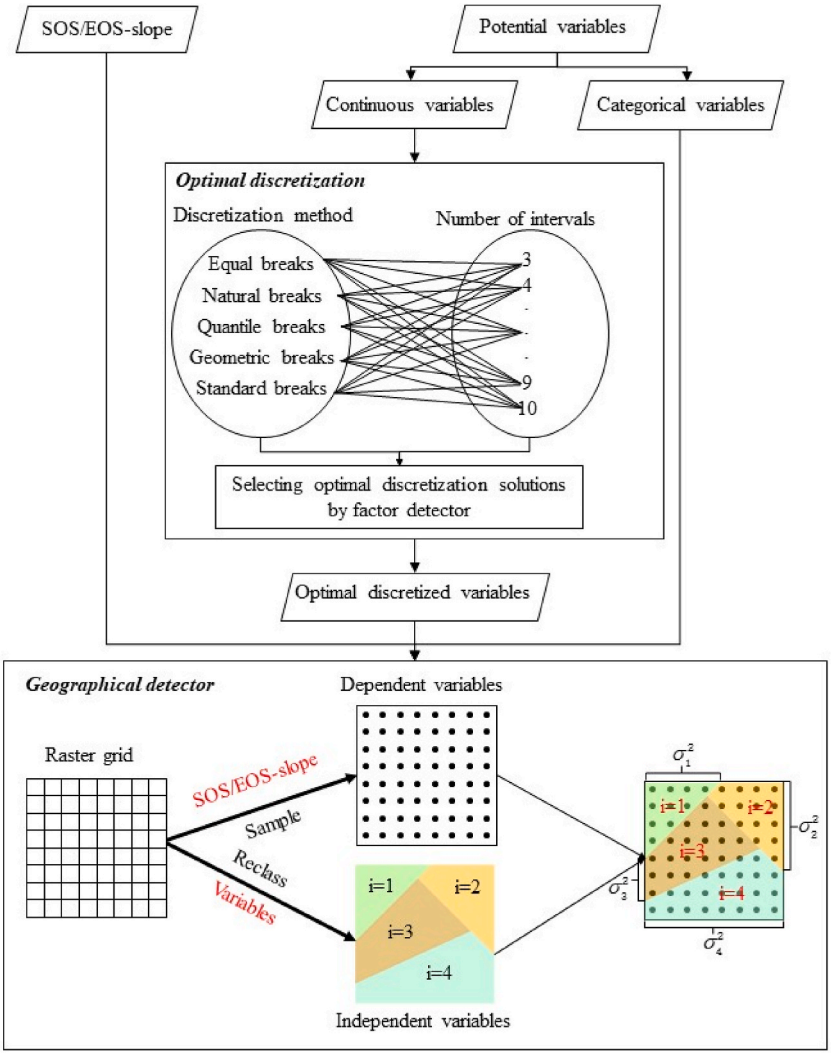

Fig. 3. The process of the GeoDetector model.

variables. The dependent variables are converted into point data by sampling. A point contains the trend of SOS and EOS, and the dependent variable is divided into *L* strata. By overlaying the independent and dependent variable strata, we can calculate the variance of the rate of change of SOS or EOS in each subregion (σ_h^2) and the variance of the study area (σ^2) to obtain Q. Q varies in the range [0,1], and the closer the value of Q is to 1, the more energy the independent variable has to explain the dependent variable, and vice versa, the weaker it is. For the GeoDetector model, the spatial scale of the data and interval division method potentially influence the Q values. The effectiveness of classifications in the GeoDetector can be evaluated using the Q statistic, with a higher Q value indicating superior partitioning outcomes [33,34,36]. Different spatial scales and divisions were used for the calculation of Q. The mean value of Q was chosen to determine the spatial scale and interval division method used in this paper.

3. Results

3.1. Spatial pattern of phenological indicators

From 2001 to 2018, the interannual SOS and EOS obtained on the TP by the TDSGM both showed a spatial variation pattern from the eastern low elevation region to the western high elevation region. For SOS, the differences in spatial distribution were even more pronounced. Compared to the western part of the study area, the eastern part, which had a lower mean elevation, exhibited significantly lower mean SOS values. Compared to SOS, the difference in spatial distribution was less pronounced for EOS. We found that EOS in the western part of the study area maintained a higher mean value overall. The earlier SOS and the later EOS were located in the eastern and western regions, respectively, ranging from 85 to 135 and 275 to 295 in Julian Day (Fig. 4a–d). We counted the mean elevation and mean SOS and EOS of different vegetation types and found that broadleaf and coniferous forests growing at lower elevations tended to experience earlier SOS, later EOS than vegetation types at higher elevations, and grassland vegetation had both later SOS and EOS, while shrubland and meadows showed later SOS, earlier EOS.

3.2. Spatiotemporal trends of SOS and EOS

According to the vegetation phenology trend (Fig. 5a–d), during the time period of 2001–2018, the SOS for vegetation on the TP exhibited a trend of advancement for the entire region at a rate of −0.36 d/10 y. However, there was some spatial variation, with the central part of the study area displaying the greatest variation. Additionally, the EOS demonstrated a weak delayed trend with an

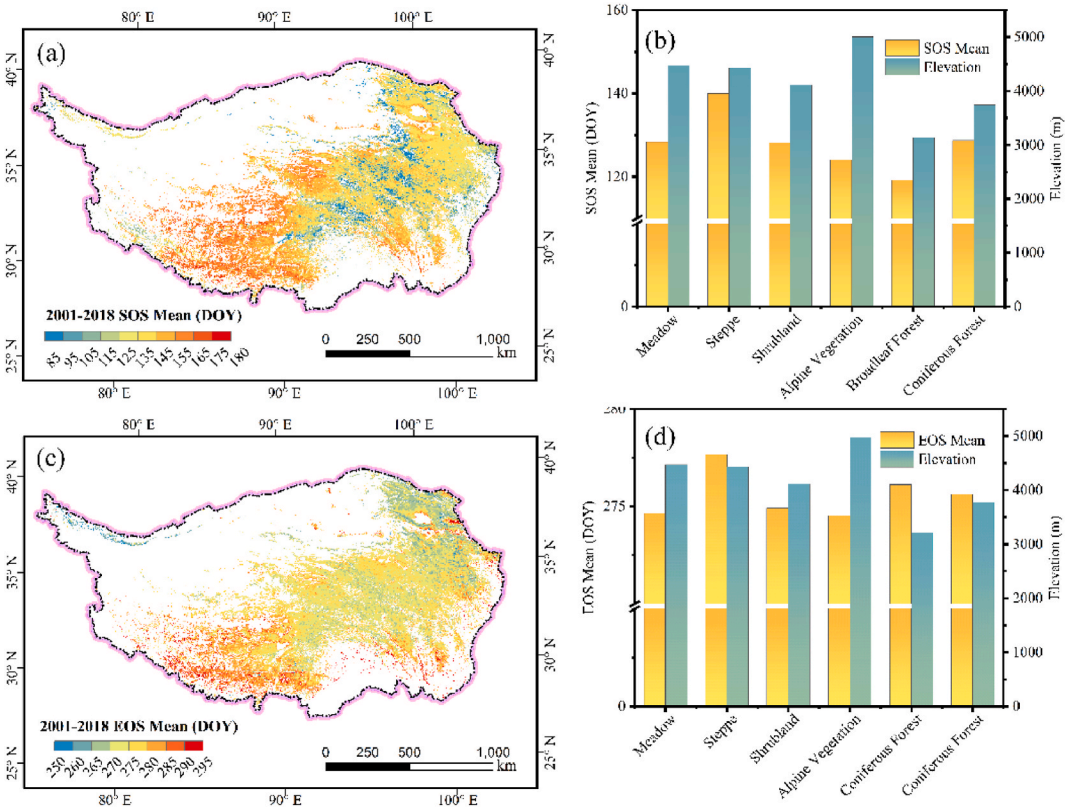

Fig. 4. Mean values of multi-year phenological metrics, SOS spatial distribution (a), SOS of different vegetation types (b), EOS spatial distribution (c), and EOS of different vegetation types (d) from 2001 to 2018.

alteration rate of approximately 0.07 d/10 y for the TP as a whole. This finding is consistent with previous studies [48,49]. In the regions where SOS was advanced, EOS also showed an advanced trend, among which in the marginal regions, EOS mainly showed a delayed situation. At the same time, the vegetation phenology trends of different vegetation types in the study area also had large variations. The general SOS of meadows remained largely unchanged, whereas the EOS exhibited a progressive trend. In contrast, both SOS and EOS of the steppe demonstrated a lagged trend. Additionally, the alpine vegetation displayed a postponed SOS trend and an advanced EOS trend. Among the forests, the broadleaf forests showed the largest EOS and SOS change rates (−0.15 d/year and 0.11 d/year), while the coniferous forests showed lower SOS and EOS change rates. This finding is consistent with Yun's results [41].

3.3. Analysis of influence factors based on GeoDetector model

The results (Fig. 6) showed that: (1) The effects of temperature and precipitation on SOS are essentially similar, with Q mean values of 0.012 and 0.013 (Fig. 6a), respectively, indicating very proximate Q values for both factors. For EOS, the Q mean value for temperature is 0.0384, while for precipitation it's 0.0135 (Fig. 6b). In this context, the influence of temperature is notably more pronounced than precipitation. However, there are significant differences in hydrothermal requirements among various vegetation types. During their growth phase, broadleaf forests are more susceptible to the influences of temperature (with a Q mean value of 0.063) and precipitation (with a Q mean value of 0.104). Conversely, for shrubs, the effects of precipitation and temperature on SOS are comparatively muted (Q mean values of 0.007 and 0.025) (Fig. 6c–e). In the later stages of vegetation growth, broadleaf forests are more sensitive to the effects of precipitation and temperature (Q mean values of 0.028 and 0.081, respectively). In contrast, coniferous forests exhibit a reduced sensitivity to changes in precipitation (Q mean value of 0.008), while alpine vegetation is less affected by temperature fluctuations (Q mean value of 0.007) (Fig. 6f–h) (2) Compared to climatic factors such as temperature and precipitation, non-climatic variables like longitude (Q value of SOS/EOS = 0.046/0.042), latitude (Q value of SOS/EOS = 0.076/0.024), and altitude (Q value of SOS/EOS = 0.031/0.030) exhibit similar or even greater influence on the distribution patterns of phenological changes. However, the effects of non-climatic variables like slope (Q value of SOS/EOS = 0.009/0.001) and aspect (Q value of SOS/EOS = 0.0002/0.0002) on vegetation can be considered negligible (Fig. 6c and f). (3) The sensitivity of SOS and EOS to climatic and non-climatic factors varies greatly, with SOS being more sensitive to changes in latitude, while the variation trend of EOS closely matches the spatial distribution of temperature.

Overall, non-climatic factors have a greater impact on SOS trends compared to climatic factors. However, the influence of non-climatic factors on SOS trends primarily stems from longitude, latitude, and elevation. The impact of slope, aspect, and soil factors is not only considerably smaller than that of longitude, latitude, and elevation, but also less than that of climatic factors. The main climatic factor affecting the change of SOS is the precipitation in spring and summer, and the temperature in winter also has a significant impact on SOS. Different vegetation types require different hydrothermal conditions. The primary climatic factor influencing the trends of SOS in alpine vegetation, broadleaf forests, and steppes is precipitation. In broadleaf forests, the contribution of spring

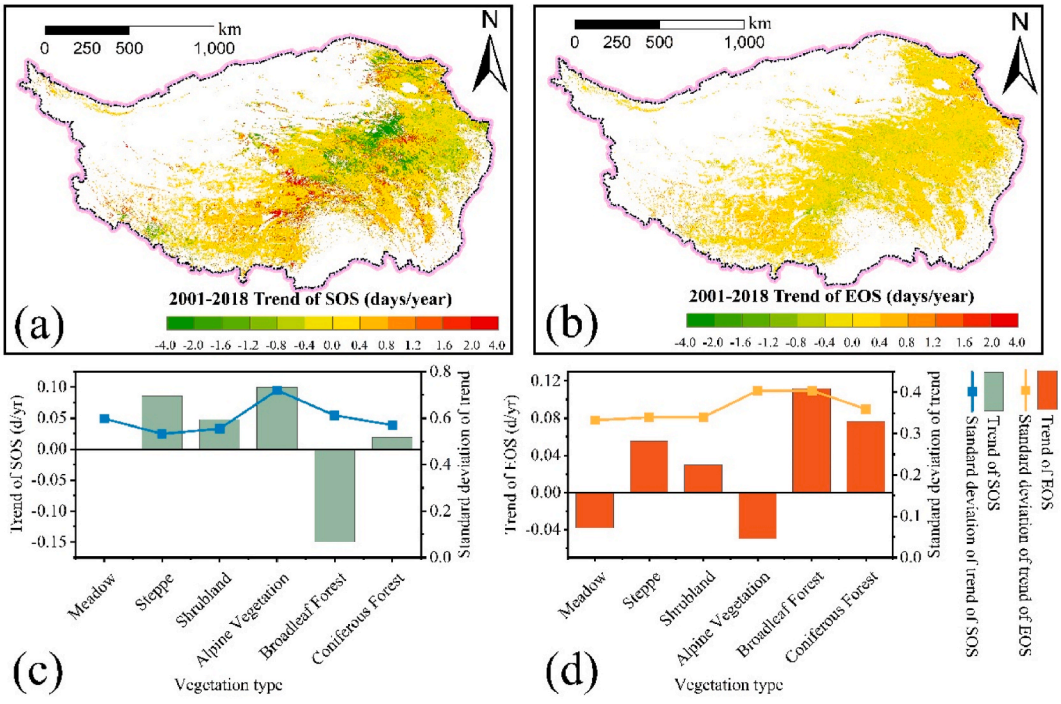

Fig. 5. Spatiotemporal trends of mean SOS (a), EOS (b) and statistics of different vegetation types (c, d). The trends of SOS and EOS represent the changes in their timing over the years. A positive value indicates an earlier SOS (EOS), while a negative value i.

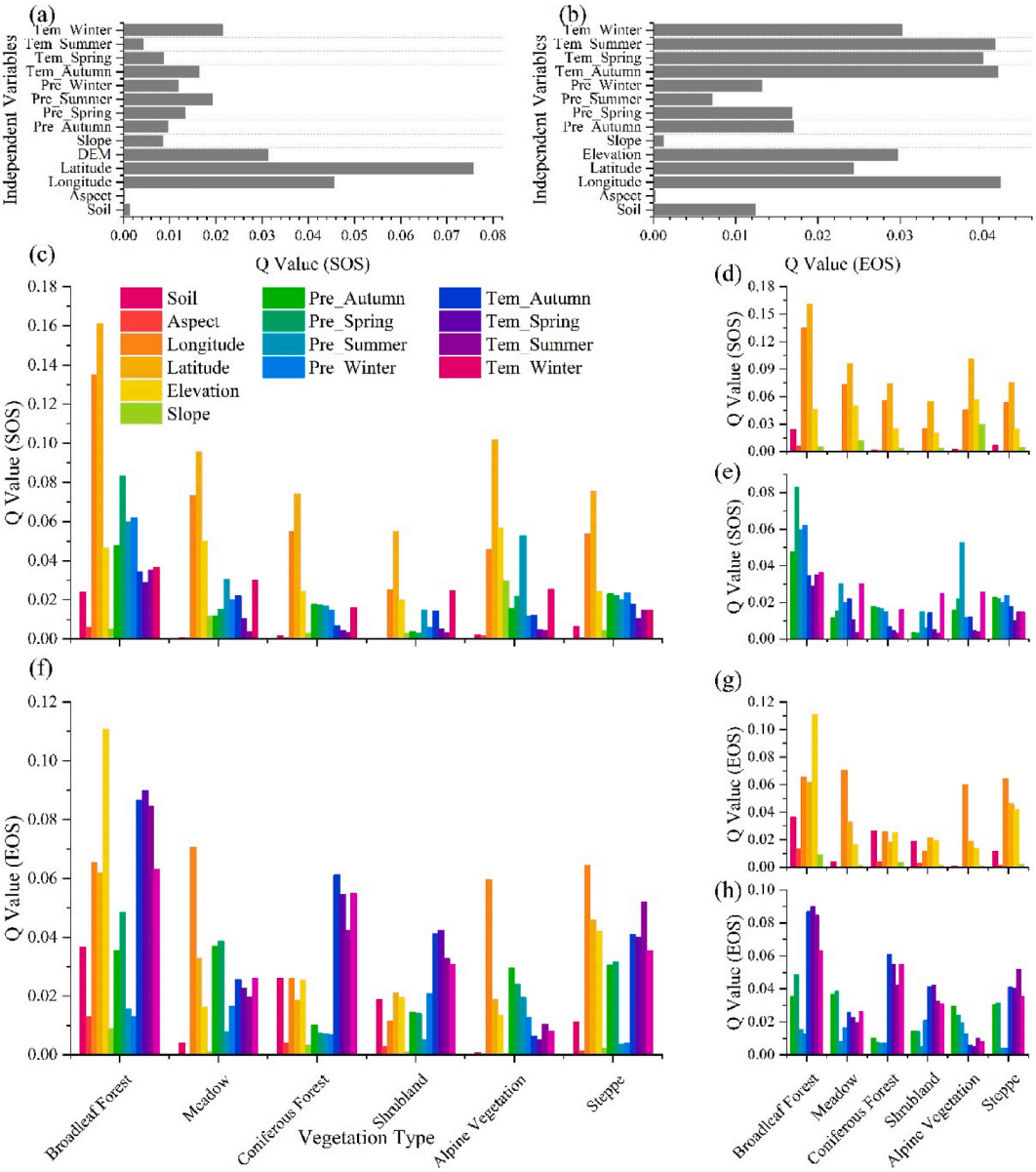

Fig. 6. Factor detection of SOS and EOS trends for overall (gray) and different types of vegetation (colored). (a)SOS, (b)EOS, (c) SOS of Climatic and Non Climatic Factors, (d) SOS of Non Climatic Factors, (e) SOS of Climatic Factors, (f) EOS of Climatic and Non Climatic Factors, (g) EOS of Non Climatic Factors, (h) EOS of Climatic Factors.

precipitation ($Q = 0.08$) is significantly greater than that of other climatic factors. Conversely, in alpine vegetation, autumn precipitation plays a more dominant role ($Q = 0.05$). In meadows and coniferous forests, the effects of temperature and precipitation on SOS show no significant differences. Winter temperature generally influences the SOS trend more than other temperatures. For scrubs, winter temperature has a greater effect on SOS than does precipitation. For meadows, coniferous forests, scrubs, and alpine vegetation, temperature's contribution to SOS variation is notably higher in winter compared to other seasons.

In contrast to SOS, climatic factors have a greater influence on EOS than non-climatic factors. Overall, the temperature is the main climatic factor driving the variability of EOS. However, EOS is still more sensitive to changes in longitude, latitude, and elevation. Compared to temperature, the EOS of meadow and alpine vegetation is more susceptible to the impact of precipitation, while the EOS of other vegetation is more susceptible to the impact of temperature. We further explored the effects of non-climatic factors such as soil type, elevation, longitude, latitude, slope and aspect on phenological changes. The contribution of longitude to EOS is usually higher, while SOS is more sensitive to the changes of latitude. In addition to latitude and longitude, elevation is also a non-climatic factor that cannot be ignored. In this study, we found that elevation has a significant impact on the SOS of alpine vegetation and the EOS of broadleaf forests.

3.4. Phenological change trend from multiple perspectives

Based on the geodetector results, factors with higher impact were selected for further analysis. The phenological trend distribution in different intervals of factors was obtained (Fig. 7).

Using the geodetector, the factors were ranked according to their effect on SOS change trend in the following order:

Latitude > Longitude > Elevation > Winter temperature > Summer precipitation > Autumn temperature > Spring precipitation > Winter precipitation > Autumn precipitation > Spring temperature > Slope > Summer temperature > Soil type > Aspect.

Among the above analysis, SOS change trends are highly influenced by latitude, longitude, elevation, winter temperature and summer precipitation, and climate factors in different seasons have similar effects on the distribution of SOS change trends. Therefore, we mainly explore SOS change trends within different value intervals of latitude, longitude, elevation, winter temperature and summer precipitation.

The results showed that there are significant differences in the trends of phenological changes between the various value ranges of the influence factors. On the TP, the SOS trend was delayed at the low-latitude regions (Latitude<32.7 °N), and the highest SOS delay (0.35 days yr-1) was observed at the 29.9–31.8 °N latitudes (Fig. 7a). In the high-latitude regions (Latitude>32.7 °N), the SOS trend was advanced, and the highest degree of SOS advancement (−0.37 days yr^{-1}) was observed at the 34.5–35.8 °N latitudes. The trend of SOS changes showed significant differences in different subregions of longitude (Fig. 7b). On the west side of the study area (Longitude <95.1°E), the SOS trend was greater than 0 days yr^{-1}, and the highest SOS delay rate (0.37 days yr^{-1}) was found at the 90.5–92.8°E longitude. On the eastern side of the study area (Longitude>95.1°E), the SOS trend was less than 0 days yr^{-1}, and the highest SOS advance rate (−0.41 days yr^{-1}) was found at the 97.2–99.5°E longitude. The SOS was advanced when the elevation was lower than 4790 m (Fig. 7c). The elevations range from 4200 m to 4390 m, the advance trend was the highest (−0.31 days yr^{-1}). The SOS was delayed when the elevation was greater than 4790 m. As the elevation increased, SOS became more delayed. In regions with lower winter temperatures (below −9.75 °C), SOS was advanced, and the colder the winter temperature, the more days SOS was advanced; in regions with higher winter temperatures (above −9.75 °C), SOS showed a tendency to be delayed, and the higher the winter

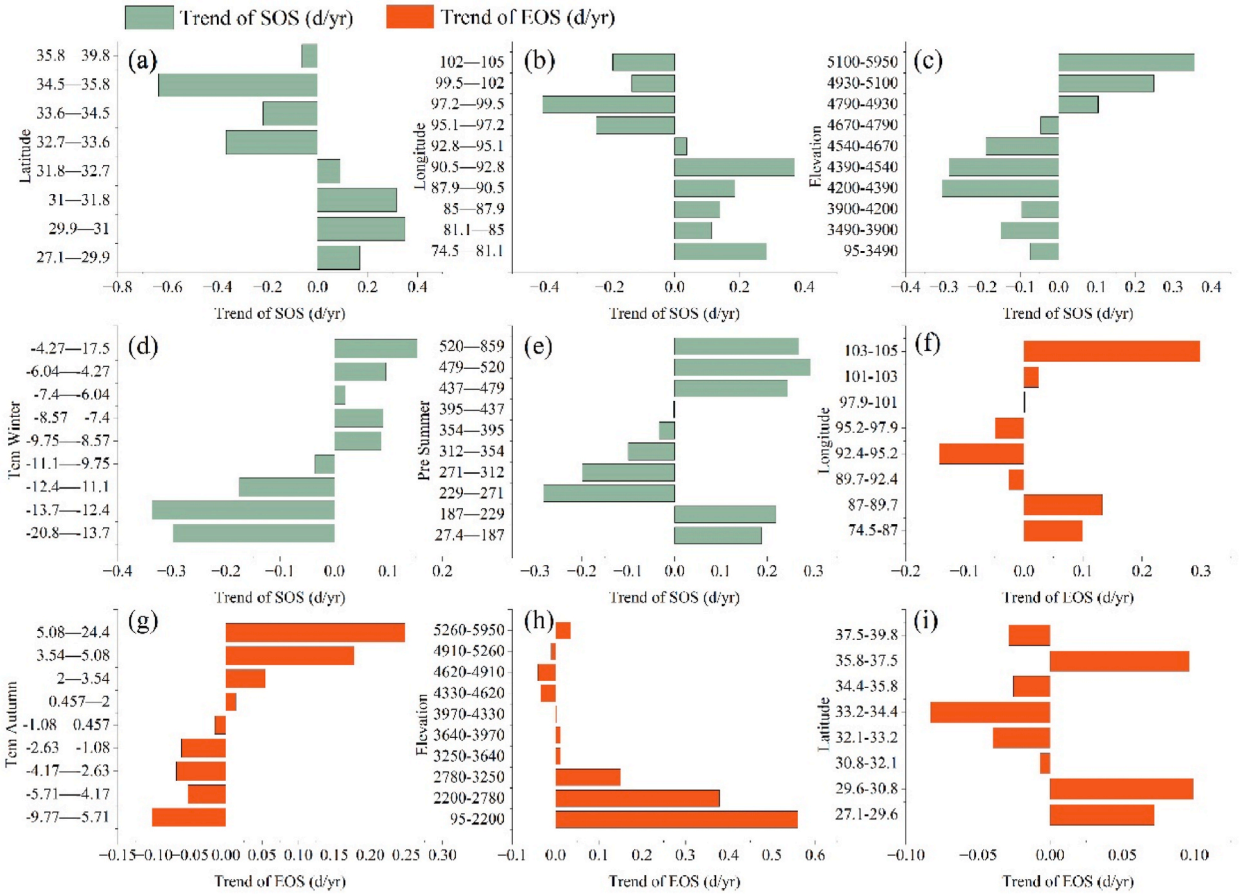

Fig. 7. Variations of SOS/EOS change rates under their dominant factors with different level (green represents the trend of SOS, red represents the trend of EOS). For abbreviations, see Table 2. (For interpretation of the references to color in this figure legend, the reader is referred to the Web version of this article.)

temperature, the more days were delayed (Fig. 7d). The SOS was delayed in areas with less (below 229 mm) and more (above 437 mm) summer precipitation, and in areas with moderate precipitation (229–437 mm), SOS was advanced (Fig. 7e).

Using the geodetector, the factors were ranked according to their effect on EOS change trend in the following order:

Longitude > Autumn temperature > Summer temperature > Spring temperature > Winter temperature > Elevation > Latitude > Autumn precipitation > Spring precipitation > Winter precipitation > Soil type > Summer precipitation > Slope > Aspect.

Among the above analysis, the influence of temperature in different seasons on the trend of EOS was relatively higher and the effect of precipitation on EOS change trend was lower. Since the climatic factors in different seasons had similar effects on the distribution of phenology, this paper mainly analyzed the influence of longitude, autumn temperature, elevation and latitude on the trend of EOS.

On the TP, from the perspective of longitude, EOS was advanced in the central region (89.7–97.7 °E) and delayed on the eastern (Longitude >97.9 °E) and western (Longitude <89.7 °E) sides, but the delay in EOS was greater on the eastern side than on the western side (Fig. 7f). The temperature in the four seasons had a similar effect on the distribution of EOS trends, which gradually changed from earlier to later as the temperature increased. The results of the autumn temperature range indicated that the EOS was gradually advanced in the lower temperature interval (below 0.46 °C) and delayed in the higher temperature interval (above 0.46 °C) (Fig. 7g). In the region with elevation lower than 4330 m, the EOS change trend was greater than 0 days yr^{-1} and showed a more obvious elevation law, i.e., the EOS change trend decreased gradually with the increase of elevation. However, the change pattern was not obvious in the higher altitude area (above 4300 m) (Fig. 7h). In contrast to SOS, the EOS trend distribution across latitudinal zones lacked a consistent pattern. This phenomenon was also consistent with the conclusion that EOS trends distribution was less influenced by latitude (Fig. 7i).

4. Discussion

4.1. Spatio-temporal patterns of SOS and EOS

Comparing the phenological parameters extracted by the different methods with the field data, we observed that the SOS and EOS obtained by the remote sensing methods were generally earlier than the field data. In addition, there were significant differences in phenological parameters obtained by different methods. Yu et al. [50] reported SOS and EOS values of 110–170 and 250–310 DOY, respectively, using the asymmetric Gaussian function. Ding et al. [51] found SOS and EOS for the TP to be 120–170 and 250–300 DOY using a combined method. Another study [52] using a 20 % and 80 % threshold reported SOS and EOS for TP meadows as 130–170 and 250–280 DOY, respectively. The alpine grassland's average SOS and EOS from 2001 to 2018 were 140–160 and 255–275 DOY [53]. This study used TDSGM to extract the vegetation phenology indicators, and the results were generally consistent with those obtained by previous researchers and were verified by comparison of site dates [54–57]. This suggests that the use of phenological extraction methods in this study is reasonable on the TP.

There was significant evidence suggesting that SOS had occurred earlier and EOS had been delayed [54–57]. However, this study revealed that vegetation phenology trends on the TP between 2001 and 2018 were much smaller than previously believed [51,53]. Moreover, the changes in EOS trends were more nuanced in comparison to SOS, with mean rates of −0.36 days per year and 0.07 days per year for both SOS and EOS, respectively (Fig. 5). These results were also confirmed by the latest research [42,57,58]. Meanwhile, the research found that SOS and EOS on the TP had strong spatial distribution characteristics, i.e., vegetation phenology showed a trend of gradual postponement from south to north. The trends of SOS and EOS exhibited vertical zonation, along with distinct latitudinal and longitudinal zonal patterns. Previous research indicated that climate predominantly influences vegetation distribution through heat and moisture conditions. Specifically, heat provides the essential energy for vegetation growth, while precipitation plays a fundamental role in phenology [59]. Climatic factors have a driving effect on the change of vegetation phenology. In the study area, temperature and precipitation decrease with increasing latitude, and precipitation increases with increasing longitude. The changes in longitude have a significant impact on the rainy season in the northwest and southern regions of the TP. These findings indicated that the trend of SOS changed from being delayed to advancing as latitude and longitude increased, while it changed from advancing to delayed with increasing elevation. The trend of EOS was more complicated, with the change of latitude, longitude, and elevation, the trend of EOS showed a U-shaped change. With the increase of longitude, latitude, and elevation, the trend of EOS changed from delayed to advanced, and then from advanced to delayed. In general, the SOS variation was smoother in the lower latitudes of the TP, but the EOS variation was smoother in the higher latitudes. The interannual variation of EOS is relatively minor across the entire TP, but it is more pronounced in specific local areas.

4.2. Response of vegetation phenology to climatic and non-climatic factors

Since the sensitivity of vegetation phenology to climate change may vary by vegetation type, it is necessary to consider the influence of climate factors on the phenology of different vegetation types [22,60,61]. The changes in SOS were attributed to the preceding year's winter temperature and summer precipitation. In regions with lower winter temperatures, vegetation exhibited an advanced SOS trend, whereas in areas with higher winter temperatures, a delayed SOS trend was observed. (Fig. 7). With increasing summer precipitation, SOS initially advanced and then subsequently delayed. The seasons in which climatic factors had the most significant impact on SOS varied depending on vegetation types. Similar studies showed that vegetation SOS in most of the Northern Hemisphere is closely related to pre-season temperatures [62]. The SOS was more sensitive to the winter temperature of the previous year on the TP. The SOS in areas with lower winter temperatures show a tendency to be delayed. This is due to lower local temperatures and freezing temperatures that can damage plant cell architecture. To avoid and minimize stress caused by cold temperatures, plants

must slow or delay developmental processes and limit physiological processes such as germination, growth, and leaf expansion. The primary form of precipitation in early spring on the TP is snowfall. The water needed for plant growth comes primarily from melting snow and ice. Freezing temperatures freeze water in the soil, making it difficult for plant roots to obtain water. As a result, compared to warm regions, SOS in cold regions is later. However, the global temperature rise has led to significant changes in the climate of TP [54–57]. Specifically, temperature variations in colder regions now have a more potent and favorable influence on the growth of indigenous vegetation. Consequently, an upward trend of SOS has emerged in the cold regions of this region.

The temperature is the main climatic factor affecting EOS, which is gradually delayed as the temperature rises (Fig. 7). Compared with temperature, rainfall has a smaller effect on EOS. The effect of precipitation on vegetation EOS is higher in spring and autumn than in other seasons. Areas with lower precipitation in spring and fall have a tendency for EOS to be delayed. Areas with higher precipitation have a tendency for EOS to advance. The period of precipitation affecting EOS is mainly concentrated in the spring and autumn of the year. Except for meadows and alpine vegetation, EOS is more susceptible to precipitation. On the TP, the EOS variation of most vegetation is mainly influenced by temperature. The EOS of the steppe is more dependent on summer temperature and the coniferous forest is more influenced by autumn temperature, while the broadleaf forest and scrub are more influenced by spring and autumn temperatures. Meanwhile, the increase in temperature delayed EOS in most parts of the TP, EOS is more sensitive to changes in temperature in summer and autumn. Moreover, plant leaves wilt earlier in the eastern and central parts of the TP despite the increase in temperature in autumn.

In addition, the influence of non-climatic factors on the changes of vegetation phenology is also a point of interest. On the TP, differences in longitude, latitude, and elevation among the non-climatic factors greatly influence the distribution of SOS trends. These three non-climatic factors have a higher influence on SOS than climatic factors, while other non-climatic factors have a lower influence on SOS. For the distribution of EOS trends, slope, aspect, and soil type are less influential. The influence of longitude is greater, higher than that of climate factors, while the influence of latitude and altitude is higher, but lower than that of climate factors. There may be two reasons why longitude, latitude, and altitude have a higher impact on vegetation phenology changes. On one hand, it was shown that latitude and altitude had a significant influence on temperature variation [64]. On the other hand, precipitation exhibited a clear trend of decreasing gradually from east to west, while elevation also increased gradually in the same direction [65]. Studies showed that changes in temperature and precipitation significantly affected vegetation phenology. On the TP, where the hydrothermal condition is at biologically limiting levels and the ecosystem is extremely fragile, a smaller change in water and heat conditions may lead to a larger fluctuation in phenology [66, 67]. Such a mixture of influences may result in the distribution of vegetation phenology trends in the region being influenced not only by climatic factors but also by longitude, latitude, and elevation.

4.3. Limitations and uncertainties

Some of the data and methods used in this study may lead to uncertainty in the results. Firstly, the climate dataset was provided by National Ecosystem Science Data Center. The climate data in this dataset, obtained from meteorological stations in and around the TP were interpolated into raster data by ANUSPLIN software [68]. However, the interpolation results, may have resulted in some uncertainties. Secondly, in order to maintain consistency with the spatial resolution of climate data, the DEM data was resampled to 500 m, which may weaken the impact of slope and aspect on vegetation phenological trends. Temperature and precipitation have been the main climatic factors used to study vegetation phenology in related studies. However, a range of climatic factors such as snowfall, soil moisture, sunshine duration and various extreme weather conditions may also have a significant impact on vegetation phenology. For example, snowfall and soil moisture directly influence the availability of water to plants, while sunshine duration affects the efficiency of photosynthesis. Apart from climatic factors, the impact of human activities (e.g., grazing, reclamation, etc.) on vegetation phenology is noteworthy. Therefore, future research should provide a comprehensive and quantitative analysis of the effects of various environmental factors on vegetation phenology. To ensure a more encompassing selection of environmental factors impacting vegetation phenology, future studies will leverage ‘bibliometric analysis’ as a reference, guaranteeing the inclusion of the most critical and influential factors.

5. Conclusion

This study analyzed the effects of climate and non-climate factors on vegetation phenology on the TP during 2001–2018. We applied the GeoDetector model to quantitatively analyze the impact of distinct environmental factors on the phenology trend of vegetation. The results revealed that SOS and EOS respond differently to climatic and non-climatic factors. Specifically, SOS variation is influenced more by latitude, longitude, and elevation, while EOS is predominantly affected by seasonal temperatures. The significance of temperature and precipitation for plants varies across different phases of the growing season. Among non-climatic factors, latitude, longitude, and altitude exert significant effects on vegetation phenology, whereas the influences of slope and aspect on plant growth are relatively subtle. Understanding how environmental differences affect vegetation phenological changes can help build more inclusive vegetation phenological models, which are crucial for predicting vegetation growth in complex environments.

Data availability statement

The data utilized in this study originates from publicly available datasets. Readers and researchers can access the original datasets from the provided references or links. Specific details related to the datasets used have been included in the ’ Materials and methods ’ section of this manuscript. Among them, the NDVI dataset product was obtained through the NASA Land Processes Distributed Active

Archive Center (NLPDAAC, http://LPDAAC.usgs.gov). The climate dataset was derived from the spatially interpolated dataset of 1 km per 8 days fine gridded meteorological data nationwide published by National Ecosystem Science Data Center, National Science & Technology Infrastructure of China (http://www.nesdc.org.cn). The soil texture dataset and the vegetation type dataset were obtained from the National Tibetan Plateau Data Center (http://data.tpdc.ac.cn).

CRediT authorship contribution statement

Xianglin Huang: Conceptualization, Data curation, Formal analysis, Investigation, Methodology, Visualization, Writing – original draft, Writing – review & editing. **Ru An:** Conceptualization, Methodology, Supervision, Writing – review & editing. **Huilin Wang:** Data curation, Methodology, Supervision, Writing – review & editing. **Fei Xing:** Data curation. **Benlin Wang:** Formal analysis. **Mengyao Fan:** Methodology. **Yunying Fang:** Supervision. **Hongliang Lu:** Methodology.

Declaration of competing interest

The authors declare that they have no known competing financial interests or personal relationships that could have appeared to influence the work reported in this paper.

Acknowledgements

This study was supported by Postgraduate Research & Practice Innovation Program of Jiangsu Province (KYCX22_0664), the National Natural Science Foundation of China (No. 41871326). We would like to express our gratitude to National Tibetan Plateau Data Center (http://data.tpdc.ac.cn) and National Ecosystem Science Data Center, National Science & Technology Infrastructure of China (http://www.nesdc.org.cn), which generously provided the Plant functional types map in China (1 km) and the interpolated temperature and precipitation dataset at 1 km grid resolution in China (2000–2018). Their contributions to the datasets were critical to the success of our study, and we appreciate their efforts in data collection and sharing. We express our heartfelt gratitude to Xiangyu Liu and Fei Xing for their valuable comments, and Yongze Song for his suggestions on the article model. We are thankful to anonymous reviewers and editor for their constructive and thoughtful inputs in this article.

References

[1] G. Zhang, et al., Green-up dates in the Tibetan Plateau have continuously advanced from 1982 to 2011, Proc. Natl. Acad. Sci. USA 110 (11) (2013) 4309–4314.
[2] N.M. Schmidt, et al., Little directional change in the timing of Arctic spring phenology over the past 25 years, Curr. Biol. 33 (15) (2023) 3244–3249.e3.
[3] S. Shi, P. Yang, C. van der Tol, Spatial-temporal dynamics of land surface phenology over Africa for the period of 1982–2015, Heliyon 9 (6) (2023), e16413.
[4] T.H. Sparks, A. Menzel, Observed changes in seasons: an overview, Int. J. Climatol. 22 (14) (2002) 1715–1725.
[5] R.I. Bertin, Plant phenology and distribution in relation to recent climate change, J. Torrey Bot. Soc. 135 (1) (2008) 126–146.
[6] R. Singh, et al., Phenological variations in relation to climatic variables of moist temperate forest tree species of western Himalaya, India, Heliyon 9 (6) (2023), e16563.
[7] M.A. White, et al., Intercomparison, interpretation, and assessment of spring phenology in North America estimated from remote sensing for 1982–2006, Global Change Biol. 15 (10) (2009) 2335–2359.
[8] Y. Xu, et al., Improving extraction phenology accuracy using SIF coupled with the vegetation index and mapping the spatiotemporal pattern of bamboo forest phenology, Rem. Sens. Environ. 297 (2023), 113785.
[9] D. Lloyd, A phenological classification of terrestrial vegetation cover using shortwave vegetation index imagery, Int. J. Rem. Sens. 11 (12) (2007) 2269–2279.
[10] J. Cao, et al., Investigating mangrove canopy phenology in coastal areas of China using time series Sentinel-1/2 images, Ecol. Indicat. 154 (2023), 110815.
[11] M.D. Schwartz, B.C. Reed, M.A. White, Assessing satellite-derived start-of-season measures in the conterminous USA, Int. J. Climatol. 22 (14) (2002) 1793–1805.
[12] F. Yu, et al., Response of seasonal vegetation development to climatic variations in eastern central Asia, Rem. Sens. Environ. 87 (1) (2003) 42–54.
[13] X. Zhang, et al., Monitoring vegetation phenology using MODIS, Rem. Sens. Environ. 84 (3) (2003) 471–475.
[14] P. Jönsson, L. Eklundh, TIMESAT—a program for analyzing time-series of satellite sensor data, Comput. Geosci. 30 (8) (2004) 833–845.
[15] Y. Chen, et al., Spatial heterogeneity of vegetation phenology caused by urbanization in China based on remote sensing, Ecol. Indicat. 153 (2023), 110448.
[16] Y. Yang, F. Fan, Land surface phenology and its response to climate change in the Guangdong-Hong Kong-Macao Greater Bay Area during 2001–2020, Ecol. Indicat. 154 (2023), 110728.
[17] A. Jacquin, D. Sheeren, J. Lacombe, Vegetation cover degradation assessment in Madagascar savanna based on trend analysis of MODIS NDVI time series, Int. J. Appl. Earth Obs. Geoinf. 12 (2010) S3–S10.
[18] D. He, et al., Tempo-differentially selected growth rate model development and improved extraction of remotely sensed phenology in the Qinghai–Tibet Plateau, J. Appl. Remote Sens. 16 (1) (2022) 18501, 18501.
[19] W. Yan, et al., Droughts force temporal change and spatial migration of vegetation phenology in the northern Hemisphere, Agric. For. Meteorol. 341 (2023), 109685.
[20] I. Chuine, Why does phenology drive species distribution? Phil. Trans. Biol. Sci. 365 (1555) (2010) 3149–3160.
[21] S. Piao, et al., Variations in satellite-derived phenology in China's temperate vegetation, Global Change Biol. 12 (4) (2006) 672–685.
[22] Y.H. Fu, et al., Declining global warming effects on the phenology of spring leaf unfolding, Nature 526 (7571) (2015) 104–107.
[23] X. Chen, et al., Modeling greenup date of dominant grass species in the Inner Mongolian Grassland using air temperature and precipitation data, Int. J. Biometeorol. 58 (4) (2014) 463–471.
[24] X. Zhang, et al., Monitoring the response of vegetation phenology to precipitation in Africa by coupling MODIS and TRMM instruments, J. Geophys. Res. Atmos. 110 (D12) (2005).
[25] W. Cheng, Z. Li, L. Yan, Uniforming spring phenology under non-uniform climate warming across latitude in China, Sci. Total Environ. 762 (2021), 143177.
[26] S. Xu, et al., Trends in evapotranspiration and their responses to climate change and vegetation greening over the upper reaches of the Yellow River Basin, Agric. For. Meteorol. 263 (2018) 118–129.
[27] J. Du, et al., Interacting effects of temperature and precipitation on climatic sensitivity of spring vegetation green-up in arid mountains of China, Agric. For. Meteorol. 269–270 (2019) 71–77.
[28] Z. He, et al., Assessing temperature sensitivity of subalpine shrub phenology in semi-arid mountain regions of China, Agric. For. Meteorol. 213 (2015) 42–52.

[29] M. Gao, et al., Divergent changes in the elevational gradient of vegetation activities over the last 30 years, Nat. Commun. 10 (1) (2019) 2970.
[30] X. Shen, et al., Asymmetric effects of daytime and nighttime warming on spring phenology in the temperate grasslands of China, Agric. For. Meteorol. 259 (2018) 240–249.
[31] N. Cong, et al., Spring vegetation green-up date in China inferred from SPOT NDVI data: a multiple model analysis, Agric. For. Meteorol. 165 (2012) 104–113.
[32] S. Liang, H. Fang, Quantitative analysis of driving factors in soil erosion using geographic detectors in Qiantang River catchment, Southeast China, J. Soils Sediments 21 (1) (2021) 134–147.
[33] Y. Song, et al., Segment-based spatial analysis for assessing road infrastructure performance using monitoring observations and remote sensing data, Rem. Sens. 10 (11) (2018) 1696.
[34] P. Luo, et al., Identifying determinants of spatio-temporal disparities in soil moisture of the Northern Hemisphere using a geographically optimal zones-based heterogeneity model, ISPRS J. Photogrammetry Remote Sens. 185 (2022) 111–128.
[35] Y. Sun, et al., Quantitative Assessment of the Impact of Climatic Factors on Phenological Changes in the Qilian Mountains, China, vol. 499, Forest Ecology and Management, 2021, 119594.
[36] J.F. Wang, et al., Geographical detectors-based health risk assessment and its application in the neural tube defects study of the heshun region, China, Int. J. Geogr. Inf. Sci. 24 (1) (2010) 107–127.
[37] G. Zhang, et al., Green-up dates in the Tibetan Plateau have continuously advanced from 1982 to 2011, Proc. Natl. Acad. Sci. USA 110 (11) (2013) 4309–4314.
[38] S. Kang, et al., Review of climate and cryospheric change in the Tibetan Plateau, Environ. Res. Lett. 5 (1) (2010), 015101.
[39] S. Wang, et al., Complex responses of spring alpine vegetation phenology to snow cover dynamics over the Tibetan Plateau, China, Sci. Total Environ. 593–594 (2017) 449–461.
[40] Q. Zhang, et al., Dynamic vulnerability of ecological systems to climate changes across the Qinghai-Tibet Plateau, China, Ecol. Indicat. 134 (2022), 108483.
[41] Y. Sun, et al., Quantitative Assessment of the Impact of Climatic Factors on Phenological Changes in the Qilian Mountains, China, vol. 499, Forest Ecology and Management, 2021, 119594.
[42] Y. Zhu, et al., Effects of data temporal resolution on phenology extractions from the alpine grasslands of the Tibetan Plateau, Ecol. Indicat. 104 (2019) 365–377.
[43] J. Van Buskirk, E. Cereghetti, J.S. Hess, Is bigger really better? Relative and absolute body size influence individual growth rate under competition, Ecol. Evol. 7 (11) (2017) 3745–3750.
[44] A. Pal, et al., Evolution of model specific relative growth rate: its genesis and performance over Fisher's growth rates, J. Theor. Biol. 444 (2018) 11–27.
[45] F.F. Blackman, P. Parija, Analytic studies in plant respiration. I.—The respiration of a population of senescent ripening apples, Proceedings of the Royal Society of London. Series B, Containing Papers of a Biological Character 103 (726) (1928) 412–445.
[46] Q. Liu, et al., Temperature, precipitation, and insolation effects on autumn vegetation phenology in temperate China, Global Change Biol. 22 (2) (2016) 644–655.
[47] R. Cao, et al., Modeling vegetation green-up dates across the Tibetan Plateau by including both seasonal and daily temperature and precipitation, Agric. For. Meteorol. 249 (2018) 176–186.
[48] N. Cong, M. Shen, S. Piao, Spatial variations in responses of vegetation autumn phenology to climate change on the Tibetan Plateau, J. Plant Ecol. 10 (5) (2017) 744–752.
[49] Q. Sun, et al., Declined trend in herbaceous plant green-up dates on the Qinghai–Tibetan Plateau caused by spring warming slowdown, Sci. Total Environ. 772 (2021), 145039.
[50] L.S. Yu, et al., Vegetation phenology in the Tibetan plateau using MODIS data from 2000 to 2010, Remote Sens. Inf. 29 (6) (2014).
[51] Y.Q. Li, Y. Jian, Phenological changes of grassland vegetation and its response to climate change in Qinghai-Tibet Plateau, Chin. J. Grassl. 43 (9) (2021).
[52] X. Zhang, et al., Effects of climate change on the growing season of alpine grassland in Northern Tibet, China, Global Ecology and Conservation 23 (2020), e01126.
[53] H. Liu, et al., Management practices should be strengthened in high potential vegetation productivity areas based on vegetation phenology assessment on the Qinghai-Tibet Plateau, Ecol. Indicat. 140 (2022), 108991.
[54] N. Cong, et al., Little change in heat requirement for vegetation green-up on the Tibetan Plateau over the warming period of 1998–2012, Agric. For. Meteorol. 232 (2017) 650–658.
[55] B. Seyednasrollah, et al., Leaf phenology paradox: why warming matters most where it is already warm, Rem. Sens. Environ. 209 (2018) 446–455.
[56] H. Sun, et al., Contrasting vegetation response to climate change between two monsoon regions in Southwest China: the roles of climate condition and vegetation height, Sci. Total Environ. 802 (2022), 149643.
[57] H. Yu, et al., Seasonal response of grasslands to climate change on the Tibetan Plateau, PLoS One 7 (11) (2012), e49230.
[58] J.A. Shao, Y. Li, J. Ni, The characteristics of temperature variability with terrain, latitude and longitude in Sichuan-Chongqing Region, J. Geogr. Sci. 22 (2) (2012) 223–244.
[59] T.M. Bafitlhile, Y. Liu, Temperature contributes more than precipitation to the greening of the Tibetan Plateau during 1982–2019, Theor. Appl. Climatol. 147 (3–4) (2022) 1471–1488.
[60] N. Chen, et al., The chained effects of earlier vegetation activities and summer droughts on ecosystem productivity on the Tibetan Plateau, Agric. For. Meteorol. 321 (2022), 108975.
[61] E.L.J.X. Haiying Yu, Winter and Spring Warming Result in Delayed Spring Phenology on the Tibetan Plateau, Proc Natl Acad Sci U S A, 2010.
[62] W.J.Y.H. Wang Junbang (Ed.), An Interpolated Temperature and Precipitation Dataset at 1-km Grid Resolution in China (2000-2018), vol. 2, China Scientific Data, 2017.